npj | Quantum Materials

www.nature.com/npjquantmats

ARTICLE OPEN

Pressure-induced superconductivity in the three-dimensional topological Dirac semimetal Cd_3As_2

Lanpo He[1,2,6], Yating Jia[3,6], Sijia Zhang[3], Xiaochen Hong[1,2], Changqing Jin[3,4] and Shiyan Li[1,5]

The recently discovered Dirac and Weyl semimetals are new members of topological materials. Starting from them, topological superconductivity may be achieved, e.g., by carrier doping or applying pressure. Here we report high-pressure resistance and X-ray diffraction study of the three-dimensional topological Dirac semimetal Cd_3As_2. Superconductivity with $T_c \approx 2.0$ K is observed at 8.5 GPa. The T_c keeps increasing to about 4.0 K at 21.3 GPa, then shows a nearly constant pressure dependence up to the highest pressure 50.9 GPa. The X-ray diffraction measurements reveal a structure phase transition around 3.5 GPa. Our observation of superconductivity in pressurised topological Dirac semimetal Cd_3As_2 provides a new candidate for topological superconductor, as argued in a recent point contact study and a theoretical work.

npj Quantum Materials (2016) **1,** 16014; doi:10.1038/npjquantmats.2016.14; published online 23 September 2016

INTRODUCTION

In recent few years, the search for topological superconductors (TSCs) has been a hot topic in condensed matter physics.[1,2] The TSCs have a full pairing gap in the bulk and gapless surface states consisting of Majorana fermions.[1] This is in close analogy to the topological insulators (TIs), which have a full insulating gap in the bulk and gapless edge or surface states.[1] The TSC is of great importance, as it is not only a new kind of exotic superconductor but also one source of Majorana ferimons for future applications in quantum computations.[1,2]

Experimentally, the simplest way to get a candidate for TSC is to convert a TI into superconductor, by tuning the parameters such as doping or pressure. For example, by doping, $Cu_xBi_2Se_3$ and $Cu_x(PbSe)_5(Bi_2Se_3)_6$ are considered to be candidates for TSCs,[3–6] while $Sn_{1-x}In_xTe$ is considered as a candidate for topological crystalline superconductor.[7,8] Under pressure, Bi_2Te_3, Bi_2Se_3, Sb_2Te_3 and Sb_2Se_3 become superconducting, which are also regarded as candidates for TSCs.[9–14] Note that there are debates on whether these candidates are indeed TSCs,[9–17] therefore further experimental works are needed to definitely identify a TSC and manipulate the Majorana fermions on its surface.

More recently, a new kind of topological material, the three-dimensional (3D) Dirac semimetal was discovered, with examples of $SrMnBi_2$, Na_3Bi and Cd_3As_2.[18–29] As a 3D analogue to graphene, the Fermi surface of the 3D Dirac semimetal only consists of 3D Dirac points with linear energy dispersion in any momentum direction.[19,23] The exotic Fermi surface of Na_3Bi and Cd_3As_2 was confirmed by the angle-resolved photoemission spectroscopy experiments.[20–22,24–26] The compound Cd_3As_2 is of particular interests, as it is stable in air, unlike Na_3Bi. On the basis of quantum transport measurement, a non-trivial π Berry's phase is obtained, which provides bulk evidence for the existence of 3D Dirac semimetal phase in Cd_3As_2.[28,29] By symmetry breaking, this 3D Dirac semimetal may be driven to a topological insulator or Weyl semimetal.[23] More interestingly, it was predicted that topological superconductivity may be achieved in Cd_3As_2 by carrier doping,[23] but this has not been realised so far. As pressure is an effective way to induce superconductivity in TIs,[10–15] it will be very interesting to check whether superconductivity can be achieved by applying pressure on Cd_3As_2.

Here we present the resistance measurements on Cd_3As_2 single crystals under pressure up to 50.9 GPa. After an initial increase with pressure, the low-temperature resistance starts to decreases with pressure above 6.4 GPa. Superconductivity appears at 8.5 GPa with $T_c \approx 2.0$ K, and the T_c increases to about 4.0 K at 21.3 GPa, then persists to the highest pressure 50.9 GPa. A structure phase transition around 3.5 GPa is also observed by X-ray diffraction (XRD) measurements. These results suggest that Cd_3As_2 may be a new topological superconductor under high pressure.

RESULTS

Pressure-induced superconductivity

Figure 1a shows the crystal structure of Cd_3As_2.[30] The cubic Cd lattice with two vacancies resides in a face-centred cubic As lattice. Figure 1b plots a typical resistivity curve of Cd_3As_2 single crystal at 0 GPa. It is metallic and non-superconducting down to 1.5 K.

In Figure 2, the resistance curves for Cd_3As_2 single crystal under various pressures are plotted. From Figure 2a, the temperature dependence of resistance already changes to insulating behaviour ($dR/dT < 0$) at 1.1 GPa. With increasing pressure, it becomes more and more insulating until 6.4 GPa. However, upon further increasing pressure, the resistance at low temperature decreases with pressure. In Figure 2b, it becomes more and more metallic up to 32.7 GPa. Figure 2c,d) show the low-temperature part of the resistance curves above 8.5 GPa. A drop of resistance is observed below 2.0 K at 8.5 GPa, which is like a superconducting transition.

[1]State Key Laboratory of Surface Physics, Department of Physics, Fudan University, Shanghai, China; [2]Laboratory of Advanced Materials, Fudan University, Shanghai, China; [3]Beijing National Laboratory for Condensed Matter Physics, Institute of Physics, Chinese Academy of Sciences, Beijing, China; [4]Collaborative Innovation Center of Quantum Matter, Beijing, China and [5]Collaborative Innovation Center of Advanced Microstructures, Nanjing, China.
Correspondence: SJ Zhang (middleor@126.com), CQ Jin (jin@iphy.ac.cn) or SY Li (shiyan_li@fudan.edu.cn)
[6]These authors contributed equally to this work.
Received 1 July 2016; revised 18 August 2016; accepted 22 August 2016

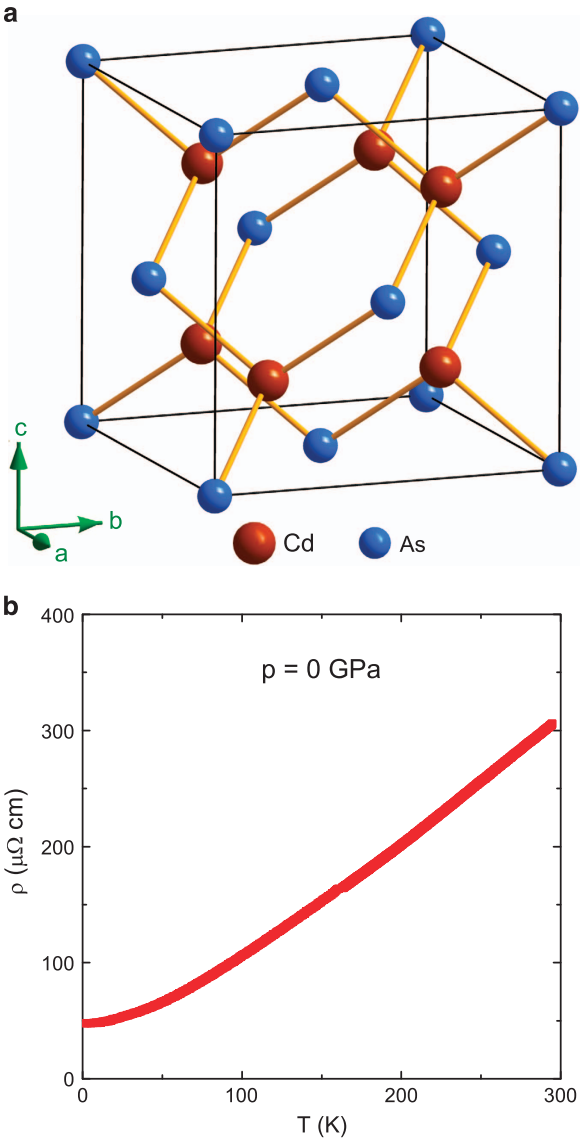

Figure 1. Crystal structure and resistivity of Cd_3As_2. (**a**) The crystal structure of Cd_3As_2. The cubic Cd lattice with two vacancies resides in a face-centred cubic As lattice. (**b**) A typical resistivity curve of Cd_3As_2 single crystal at 0 GPa.

At 11.7 GPa, the resistance drops to zero, and the transition temperature $T_c = 3.3$ K is defined at the cross of the two straight lines. The T_c increases to about 4.0 K at 21.3 GPa, then persists to the highest pressure 50.9 GPa.

To make sure the resistance drop in Figure 2 is a superconducting transition, we measure the low-temperature resistance under 13.5 GPa in magnetic fields applied perpendicular to the (112) plane, as shown in Figure 3a. The resistance drop is gradually suppressed to lower temperature with increasing field, which demonstrates that it is indeed a superconducting transition. Note that such a superconductivity we observed here is very unlikely due to contamination of pure As, as its highest T_c under pressures is much lower, and the pressure dependence of T_c is quite different.[31]

Figure 3b plots the temperature dependence of H_{c2}. Although limited by the temperature range we measured, one can see an apparently linear temperature dependence of H_{c2}. With a linear fit to the data, $H_{c2}(0) \approx 4.29$ T is roughly estimated. This value is higher than the orbital limiting field $H_{c2}^{orb}(0) = 0.72T_c|dH_{c2}/dT|_{T=T_c} = 3.71$ T, according to Werthamer–Helfand–Hohenberg formula.[32] It is much lower than the Pauli limiting field $H_P(0) = 1.84T_c = 7.89$ T,[33,34] suggesting an absence of Pauli pair breaking. The linear temperature dependence of H_{c2} in Figure 3b is actually very interesting. It may come from a two-band Fermi surface topology as in MgB_2,[35–37] or an unconventional superconducting state as in heavy-fermion compound UBe_{13}.[38] Similar linear temperature dependence of H_{c2} has recently been observed in pressurised TSC candidates Bi_2Se_3 and $Cu_xBi_2Se_3$, in natural TSC candidate Au_2Pb and in non-centrosymmetric superconductor YPtBi under ambient and high pressures, which was considered as an indication of unconventional superconducting state.[11,39–41]

We notice that no superconductivity was observed up to 13.43 GPa in an earlier pressure study of Cd_3As_2 single crystal.[42] The reason may be that their sample is slightly different from ours, and pressure higher than 13.43 GPa is needed to induce superconductivity. Interestingly, we also notice two recent point contact studies on Cd_3As_2 polycrystal and single crystal, respectively.[43,44] In both studies, indication of superconductivity was found around the point contact region on the surface, with T_c comparable to ours. In particular, no superconductivity is observed by the 'soft' point contact technique, therefore it was suggested that the superconductivity observed around the point contact region under the 'hard' tip might be induced by the local pressure.[44] In this sense, our bulk resistance measurements under hydrostatic pressure confirm pressure-induced superconductivity in Cd_3As_2, although the local pressure under the 'hard' tip is more like uniaxial stress.

Pressure-induced crystal structure phase transition

Before discussing whether the pressure-induced superconductivity is topological or not, it is important to know whether it is accompanied by a structure phase transition, as observed in pressurised TIs.[9–14] High-pressure powder XRD measurements on Cd_3As_2 were performed up to 17.80 GPa. In Figure 4, the XRD patterns below 2.60 GPa can be well indexed as the tetragonal phase in space group $I4_1/acd$.[30] All the peaks are slightly shifted to higher angle with increasing pressure, due to the shrink of the lattice. However, when the pressure increases to 4.67 GPa and above, a set of new peaks emerges, which is clearly different from that of low-pressure tetragonal phase. This abrupt change indicates that a new crystal structure phase appears, and we roughly determine the transition pressure around 3.5 GPa. Similar high-pressure XRD patterns have been observed in an earlier work, and the new high-pressure phase was determined as monoclinic in space group $P2_1/c$.[42]

The unusual T_c–p phase diagram

In Figure 5, we plot the temperature versus pressure phase diagram for Cd_3As_2. As the resistance was only measured down to 1.8 K, we cannot judge whether the superconductivity emerges at the same time as the structural transition near 3.5 GPa, or inside the high-pressure phase. Nevertheless, after increasing from 1.8 to about 4.0 K, there is apparently a region of constant T_c from 21.3 to 50.9 GPa. Such a phase diagram is very similar to that of 3D TI Bi_2Se_3, which also shows a nearly constant T_c from 30 to 50 GPa after an initial increase of T_c starting from 12 GPa.[11] A constant T_c over such a large pressure range is highly anomalous, as Kirshenbaum *et al.*[11] already pointed out. For Bi_2Se_3, two mechanisms with contrasting pressure-dependant T_c may be balanced to produce a pressure-invariant T_c over a wide range of pressure.[11] It was argued that the unique pressure evolution of T_c and the anomalous linear temperature dependence of H_{c2} are two evidences for unconventional superconductivity in Bi_2Se_3.[11] The

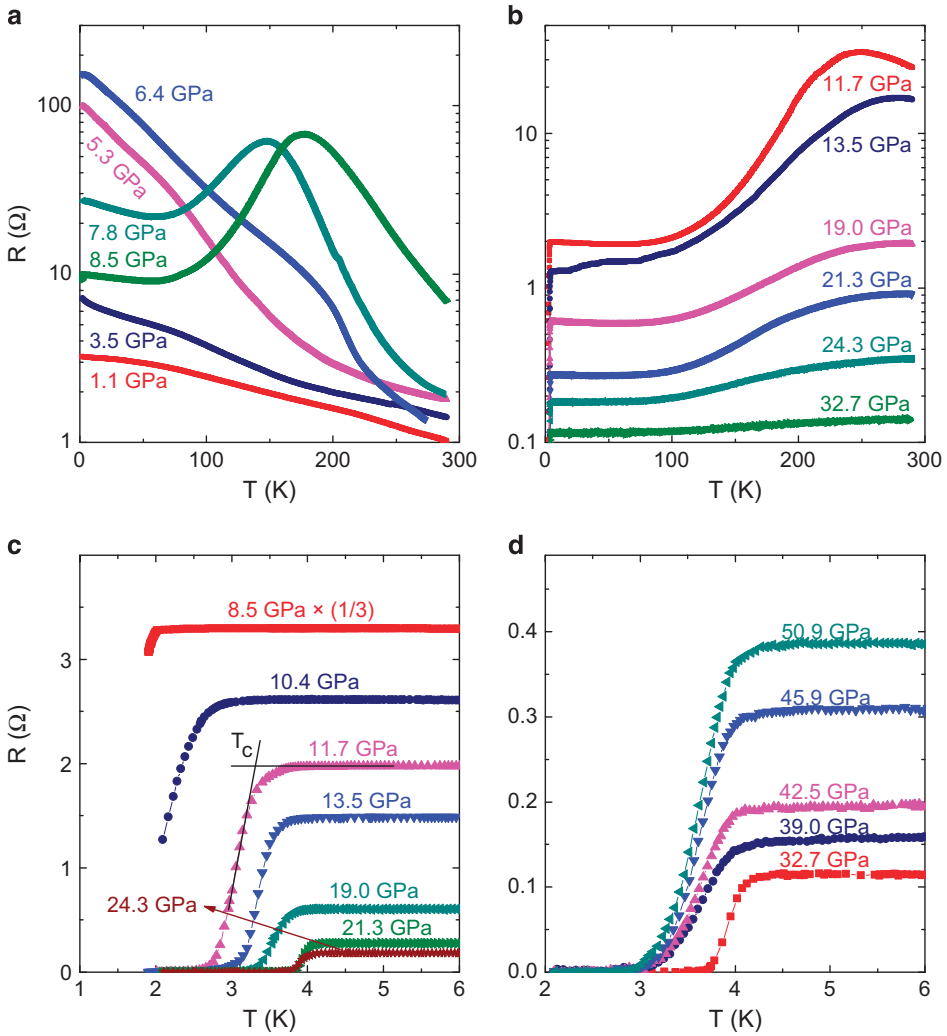

Figure 2. Experimental evidence of pressure-induced superconductivity. The temperature dependence of resistance for Cd_3As_2 single crystal under various pressures. (**a**,**b**) The resistance from 1.8 to 300 K. (**c**,**d**) Low-temperature resistance showing the superconducting transition. The superconductivity appears at $P = 8.5$ GPa with $T_c \approx 2.0$ K. The T_c is defined as on the curve of $P = 11.7$ GPa. The T_c increases to about 4.0 K at 21.3 GPa, then persists to the highest pressure 50.9 GPa.

similarity between Cd_3As_2 and Bi_2Se_3 under pressure is worthy of further investigation.

DISCUSSION

Now we discuss whether the superconducting state of Cd_3As_2 under high pressure is topological or not. In ref. 44, the observation of zero bias conductance peak and double conductance peaks under 'hard' tip reveal *p*-wave like unconventional superconductivity in Cd_3As_2. Considering its special topological property, they suggested that Cd_3As_2 under high pressure is a candidate of the TSC.[44] Furthermore, a recent theoretical work also argued that Cd_3As_2 likely realises a TSC with bulk point nodes and a surface Majorana fermion quartet.[45] Under high pressure, the symmetry-lowering effect may stabilise the TSC phase by increasing the condensation energy, as the point nodes in the TSC phase are gapped when C_4 reduces to C_2 (the structure phase transition from tetragonal to monoclinic).[45] These two works suggest that the superconductivity we observe under hydrostatic pressure is topological, although detailed band structure calculation for the high-pressure phase of Cd_3As_2 is needed to give more information about this possible TSC phase.

In summary, we have done resistance measurements on the 3D Dirac semimetal Cd_3As_2 single crystals under pressures up to 50.9 GPa. It is found that superconductivity with $T_c \approx 2.0$ K emerges at 8.5 GPa. The T_c increases to 4.0 K at 21.3 GPa, then it shows an anomalous constant pressure dependence up to the highest pressure measured. High-pressure powder XRD measurements reveal a structure phase transition around 3.5 GPa. Our observation of superconductivity in Cd_3As_2 under high pressure provides an interesting candidate for topological superconductor.

MATERIALS AND METHODS

High-quality Cd_3As_2 single crystals were grown from Cd flux.[28] The largest natural surface was determined as (112) plane by XRD. The resistivity in vacuum (0 GPa) was measured on a large sample with dimension of 1.50×0.40 mm^2 in the (112) plane and 0.15 mm in thickness. The resistance measurement under pressure between 1.1 and 50.9 GPa was performed using diamond anvil cell with solid transmitting medium

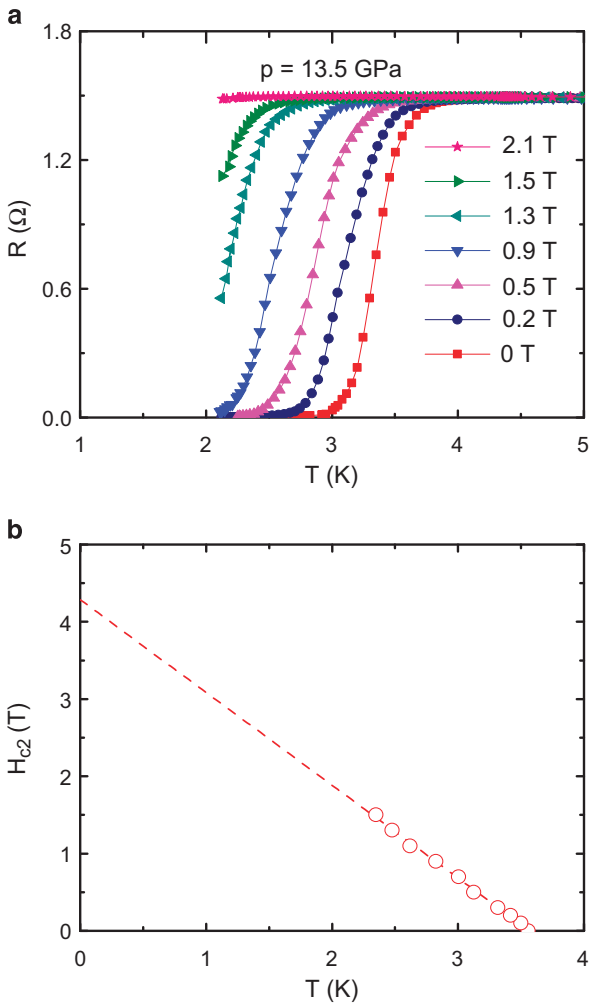

Figure 3. The upper critical field H_{c2} of Cd_3As_2 under 13.5 GPa. (**a**) The superconducting transition of the Cd_3As_2 single crystal under 13.5 GPa and in magnetic fields applied perpendicular to the (112) plane. (**b**) Temperature dependence of the upper critical field H_{c2}. The dashed line is a linear fit to the data, which points to $H_{c2}(0)\approx4.29$ T.

hexagonal boron nitride.[9,13,14] The sample size is about 80×80 μm^2 in the (112) plane, with the thickness of ~10 μm. The pressure was determined by ruby fluorescence method at room temperature before and after each cooling down. The high-pressure powder XRD measurements with synchrotron radiation were performed at the HPCAT of Advanced Photon Source of Argonne National Lab (Lemont, IL, USA) using a symmetric Mao Bell diamond anvil cell at room temperature. The X-ray wavelength is 0.434 Å.

ACKNOWLEDGEMENTS

We thank X Dai and Z Fang for helpful discussions. This work is supported by the Ministry of Science and Technology of China (No. 2012CB821402, No. 2015CB921401 and No. 2016YFA0300503), the Natural Science Foundation of China, Program for Professor of Special Appointment (Eastern Scholar) at Shanghai Institutions of Higher Learning and STCSM of China (No. 15XD1500200).

CONTRIBUTIONS

L.H. and X.H. grew the single crystals of Cd_3As_2; Y.J. and S.Z. performed the transport measurements and analysed the data; L.H. and S.L. wrote the manuscript; S.L. and C. J. supervised the project.

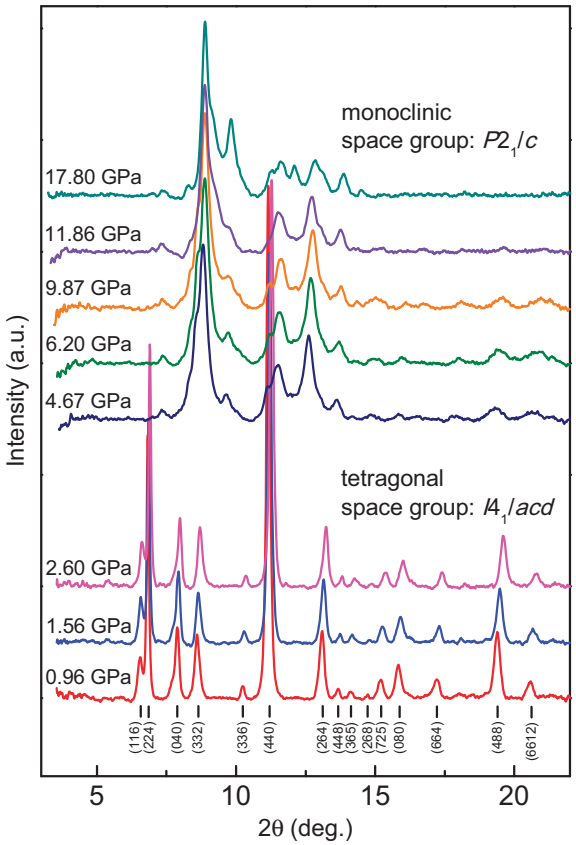

Figure 4. Crystal structure phase transition of Cd_3As_2 under pressure. The powder XRD patterns of Cd_3As_2 under different pressures at room temperature. Below 2.60 GPa, the XRD patterns can be well indexed as the tetragonal phase in space group $I4_1/acd$ (shown by short black lines). A set of new peaks emerges when increasing pressure to 4.67 GPa and above, which shows a structure phase transition from tetragonal to monoclinic phase.

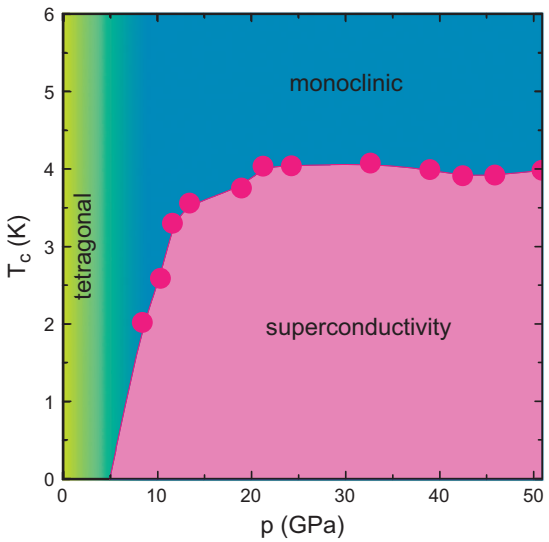

Figure 5. The phase diagram of Cd_3As_2. Temperature versus pressure phase diagram of Cd_3As_2. A structure phase transition occurs between 2.60 and 4.67 GPa. After increasing from 1.8 to about 4.0 K, there is apparently a region of constant T_c from 21.3 to 50.9 GPa. Such a phase diagram is similar to that of the 3D topological insulator Bi_2Se_3.

COMPETING INTERESTS

The authors declare no conflict of interest.

REFERENCES

1. Qi, X.-L. & Zhang, S.-C. Topological insulators and superconductors. *Rev. Mod. Phys.* **83**, 1057 (2011).
2. Ando, Y. & Fu, L. Topological crystalline insulators and topological superconductors: from concepts to materials. *Annu. Rev. Condens. Matter Phys.* **6**, 361 (2015).
3. Hor, Y. S. *et al.* Superconductivity in $Cu_xBi_2Se_3$ and its implications for pairing in the undoped topological insulator. *Phys. Rev. Lett.* **104**, 057001 (2010).
4. Das, P., Suzuki, Y., Tachiki, M. & Kadowaki, K. Spin-triplet vortex state in the topological superconductor $Cu_xBi_2Se_3$. *Phys. Rev. B* **83**, 220513 (2011).
5. Sasaki, S. *et al.* Topological superconductivity in $Cu_xBi_2Se_3$. *Phys. Rev. Lett.* **107**, 217001 (2011).
6. Sasaki, S., Segawa, K. & Ando, Y. Dirac-fermion-induced parity mixing in superconducting topological insulators. *Phys. Rev. B* **90**, 184516 (2014).
7. Sasaki, S. *et al.* Odd-parity pairing and topological superconductivity in a strongly spin-orbit coupled semiconductor. *Phys. Rev. Lett.* **109**, 217004 (2012).
8. Sato, T. *et al.* Fermiology of the strongly spin-orbit coupled superconductor $Sn_{1-x}In_xTe$: implications for topological superconductivity. *Phys. Rev. Lett.* **110**, 206804 (2013).
9. Zhang, J. L. *et al.* Pressure-induced superconductivity in topological parent compound Bi_2Te_3. *Proc. Natl Acad. Sci. USA* **108**, 24 (2011).
10. Zhang, C. *et al.* Phase diagram of a pressure-induced superconducting state and its relation to the Hall coefficient of Bi_2Te_3 single crystals. *Phys. Rev. B* **83**, 140504(R) (2011).
11. Kirshenbaum, K. *et al.* Pressure-induced unconventional superconducting phase in the topological insulator Bi_2Se_3. *Phys. Rev. Lett.* **111**, 087001 (2013).
12. Matsubayashi, K., Terai, T., Zhou, J. S. & Uwatoko, Y. Superconductivity in the topological insulator Bi_2Te_3 under hydrostatic pressure. *Phys. Rev. B* **90**, 125126 (2014).
13. Zhu, J. *et al.* Superconductivity in topological insulator Sb_2Te_3 induced by pressure. *Sci. Rep.* **3**, 2016 (2013).
14. Kong, P. P. *et al.* Superconductivity in strong spin orbital coupling compound Sb_2Se_3. *Sci. Rep.* **4**, 6679 (2014).
15. Levy, N. *et al.* Experimental evidence for *s*-wave pairing symmetry in superconducting $Cu_xBi_2Se_3$ single crystals using a scanning tunneling microscope. *Phys. Rev. Lett.* **110**, 117001 (2013).
16. Mizushima, T., Yamakage, A., Sato, M. & Tanaka, Y. Dirac-fermion-induced parity mixing in superconducting topological insulators. *Phys. Rev. B* **90**, 184516 (2014).
17. Lahoud, E. *et al.* Evolution of the Fermi surface of a doped topological insulator with carrier concentration. *Phys. Rev. B* **88**, 195107 (2013).
18. Park, J. *et al.* Anisotropic Dirac fermions in a Bi square net of $SrMnBi_2$. *Phys. Rev. Lett.* **107**, 126402 (2011).
19. Wang, Z. *et al.* Dirac semimetal and topological phase transitions in A_3Bi (A = Na, K, Rb). *Phys. Rev. B* **85**, 195320 (2012).
20. Liu, Z. K. *et al.* Discovery of a three-dimensional topological Dirac semimetal, Na_3Bi. *Science* **343**, 864 (2014).
21. Xu, S.-Y. *et al.* Observation of a bulk 3D Dirac multiplet, Lifshitz transition, and nestled spin states in Na_3Bi. Preprint at https://arxiv.org/abs/1312.7624 (2013).
22. Xu, S.-Y. *et al.* Observation of Fermi arc surface states in a topological metal. *Science* **347**, 294 (2015).
23. Wang, Z., Weng, H., Wu, Q., Dai, X. & Fang, Z. Three-dimensional Dirac semimetal and quantum transport in Cd_3As_2. *Phys. Rev. B* **88**, 125427 (2013).
24. Liu, Z. K. *et al.* A stable three-dimensional topological Dirac semimetal Cd_3As_2. *Nat. Mater.* **13**, 677 (2014).
25. Neupane, M. *et al.* Observation of a three-dimensional topological Dirac semimetal phase in high-mobility Cd_3As_2. *Nat. Commun.* **5**, 3786 (2014).
26. Borisenko, S. *et al.* Experimental realization of a three-dimensional Dirac semimetal. *Phys. Rev. Lett.* **113**, 027603 (2014).
27. Jeon, S. *et al.* Landau quantization and quasiparticle interference in the three-dimensional Dirac semimetal Cd_3As_2. *Nat. Mater.* **13**, 851 (2014).
28. He, L. P. *et al.* Quantum transport evidence for the three-dimensional Dirac semimetal phase in Cd_3As_2. *Phys. Rev. Lett.* **113**, 246402 (2014).
29. Zhao, Y. F. *et al.* Anisotropic Fermi surface and quantum limit transport in high mobility three-dimensional Dirac semimetal Cd_3As_2. *Phys. Rev. X* **5**, 031037 (2015).
30. Ali, M. N. *et al.* The crystal and electronic structures of Cd_3As_2, the three-dimensional electronic analogue of graphene. *Inorg. Chem.* **53**, 4062 (2014).
31. Chen, A. *et al.* Superconductivity in arsenic at high pressures. *Phys. Rev. B* **46**, 5523 (1992).
32. Werthamer, N. R., Helfand, E. & Hohenberg, P. C. Temperature and purity dependence of the superconducting critical field, H_{c2}. III. Electron spin and spin-orbit effects. *Phys. Rev.* **147**, 295 (1966).
33. Clogston, A. M. Upper limit for the critical field in hard superconductors. *Phys. Rev. Lett.* **9**, 266 (1962).
34. Chandrasekhar, B. S. A note on the maximum critical field of high-field superconductors. *Appl. Phys. Lett.* **1**, 7 (1962).
35. Buzea, C. & Yamashita, T. Review of the superconducting properties of MgB_2. *Supercond. Sci. Technol.* **14**, R115 (2001).
36. Gurevich, A. Enhancement of the upper critical field by nonmagnetic impurities in dirty two-gap superconductors. *Phys. Rev. B* **67**, 184515 (2003).
37. Gurevich, A. Limits of the upper critical field in dirty two-gap superconductors. *Physica C* **456**, 160 (2007).
38. Maple, M. B. *et al.* Upper critical magnetic field of the heavy-fermion superconductor UBe_{13}. *Phys. Rev. Lett.* **54**, 477 (1985).
39. Bay, T. V. *et al.* Superconductivity in the doped topological insulator $Cu_xBi_2Se_3$ under high pressure. *Phys. Rev. Lett.* **108**, 057001 (2012).
40. Xing, Y. *et al.* Superconductivity in topologically nontrivial material Au_2Pb. *npj Quant. Mater.* **1**, 16005 (2016).
41. Bay, T. V., Naka, T., Huang, Y. K. & de Visser, A. Superconductivity in noncentrosymmetric YPtBi under pressure. *Phys. Rev. B* **86**, 064515 (2012).
42. Zhang, S. *et al.* Breakdown of three-dimensional Dirac semimetal state in pressurized Cd_3As_2. *Phys. Rev. B* **91**, 165133 (2015).
43. Aggarwal, L. *et al.* Unconventional superconductivity at mesoscopic point contacts on the 3D Dirac semimetal Cd_3As_2. *Nat. Mater.* **15**, 32 (2015).
44. Wang, H. *et al.* Observation of superconductivity induced by a point contact on 3D Dirac semimetal Cd_3As_2 crystals. *Nat. Mater.* **15**, 38 (2015).
45. Kobayashi, S. & Sato, M. Topological superconductivity in Dirac semimetals. *Phys. Rev. Lett.* **115**, 187001 (2015).